Electrochimica Acta 185 (2015) 267–275

Contents lists available at ScienceDirect

Electrochimica Acta

journal homepage: www.elsevier.com/locate/electacta

Comparative study to understand the intrinsic properties of Pt and Pd catalysts for methanol and ethanol oxidation in alkaline media

Jianshe Wang[a,b,*], Niancai Cheng[b], Mohammad Norouzi Banis[b], Biwei Xiao[b], Adam Riese[b], Xueliang Sun[b,*]

[a] School of Chemical Engineering and Energy, Zhengzhou University, Zhengzhou 450000, PR China
[b] Department of Mechanical and Materials Engineering, The University of Western Ontario, ON, N6A 5B9, Canada

ARTICLE INFO

Article history:
Received 5 June 2015
Received in revised form 30 August 2015
Accepted 25 October 2015
Available online 28 October 2015

Keywords:
Pt
Pd
methanol and ethanol oxidation
deactivation
alkaline media

ABSTRACT

The understanding of the intrinsic properties of Pt and Pd is important for the rational design of catalysts for methanol and ethanol oxidation in alkaline media. In this paper, Pd catalysts, Pt catalysts and bimetallic PtPd catalysts supported on nitrogen-doped graphene are investigated. The cyclic voltammograms (CVs) for the bimetallic catalysts in 1 M KOH solution demonstrate the increasing surface composition of Pt versus Pd. The linear sweep voltammetry results show that the onset potential for OH formation on Pt is lower than on Pd, indicating that Pt has a higher affinity for OH than Pd. The CVs recorded for methanol and ethanol oxidation show that ethanol oxidation occurs at lower potentials, suggesting that ethanol is a more active fuel than methanol. Ethanol and methanol oxidation occurs at lower potentials on Pt than on Pd, revealing that Pt is intrinsically more active than Pd. Chronoamperometry results show that the rate of catalysts deactivation during ethanol oxidation is more severe compared with methanol oxidation, especially for catalysts with higher Pt content. The possible reason for the deactivation behaviors is presented and recommendations are given for future catalysts development.

1. Introduction

Direct alcohol fuel cells (DAFCs) [1–10], fuelled by low molecular weight alcohols such as methanol and ethanol at modest temperature, can provide power for automobile and portable electronics. Compared with gaseous hydrogen fuel, liquid alcohols have higher energy density [9,10] and can be easily handled, stored and transported. Furthermore, these alcohols can be directly obtained and used while pure hydrogen must be produced through complex processes involving steam reforming of hydrocarbons [11,12] or other methods such as electrochemical water-splitting [13,14]. Therefore, DAFCs have gained considerable research attention in the past decade. Most recently, alkaline direct alcohol fuel cells (ADAFCs) [4–9] have recaptured the interest of researchers because of their advantages in performance/cost and the practical feasibility offered by alkaline electrolyte membranes [15]. Specifically, in alkaline media, higher activity of alcohols oxidation and oxygen reduction can be achieved compared with acidic media, and, importantly, non-Pt materials might be used as potential catalysts in both anode and cathode to reduce the cost [8,9,15].

Methanol and ethanol are two of the most popular fuels for ADAFCs. Methanol can be cheaply produced through large-scale chemical process, and its oxidation can proceed via a more facile pathway compared with the complex C-C bond cleavage mechanism [16–18] involved in the complete oxidation of ethanol. Ethanol has a higher volumetric energy density and lower toxicity in comparison with methanol, and has been viewed as a renewable fuel because it can be produced from biomass fermentation [9]. Until now the most widely used catalysts for methanol and ethanol oxidation are Pt and Pd [5,16]. Although other materials such as Au [19,20], Ni [21] and nickel cobalt oxides [22] have also been studied, the overpotentials for alcohol oxidation on these materials are too high, which would greatly reduce the practical voltage of a working fuel cell. Pd is highly active for ethanol oxidation while less active for methanol oxidation in alkaline media [7,8]. It has been reported that Pd is even more active than Pt for ethanol oxidation judging from onset potential and peak current [6]. However, lower onset potentials for ethanol oxidation on Pt in comparison with Pd have also be demonstrated [4,5,23], and a comparative study [24] on ethanol electrooxidation on Pd and Pt has confirmed that Pt is more active than Pd for the cleavage of the á-H (a crucial step for alcohol electrooxidation). Such results

* Corresponding author. Tel.: +1 519 661 2111x87759; fax: +1 519 661 3020.
E-mail addresses: wangjs07@zzu.edu.cn (J. Wang), xsun@eng.uwo.ca (X. Sun).

http://dx.doi.org/10.1016/j.electacta.2015.10.151
0013-4686/

indicate that the evaluation of the intrinsic activity of Pd and Pt is still controversial. On the other hand, it has been widely noticed that Pd is more active for ethanol oxidation than for methanol oxidation [6–8] while Pt is prone to be poisoned during ethanol oxidation [23,25,26], but a thorough explanation for these results is still lacking.

To gain a deeper insight into the Pt and Pd properties for methanol and ethanol oxidation, in this study, we designed and prepared six catalysts with different surface composition of Pt and Pd and compared their catalytic behaviours using electrochemical methods including linear sweeping voltammetry (LSV), cyclic voltammetry (CV) and chronoamperometry. We believe the study will be beneficial for future rational catalyst design and for appropriate matching between catalysts (Pt or Pd) and fuels (methanol or ethanol).

2. Experimental

2.1. Preparation of nitrogen-doped graphene (NGN)

It has been reported that clean Pd nanoparticles can be deposited spontaneously on nitrogen-doped graphene nanosheet (NGN) due to the appropriate reducing ability of NGN [27,28]. Furthermore, NGN can also improve the anchoring stability and activity of Pt catalysts in comparison with graphene nanosheets

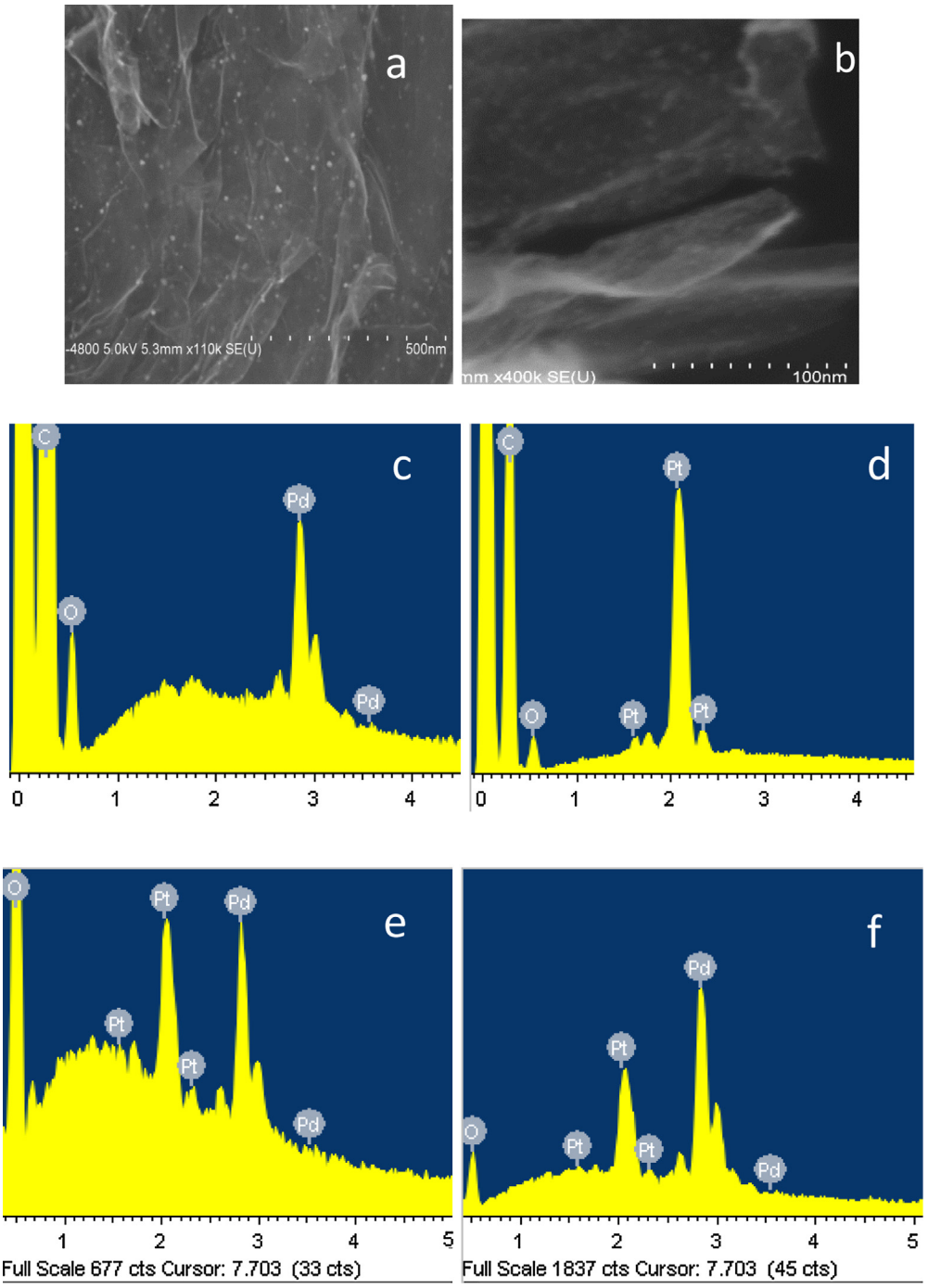

Fig. 1. (a) SEM image for NGN/Pd; (b) SEM image for NGN/Pt; (c) EDX spectra for NGN/Pd; (d) EDX spectra for NGN/Pt; (e) EDX spectra for NGN/PdPt-1; (f) EDX spectra for NGN/PdPt-2.

[29]. Therefore, we used NGN as both reducing agent and support for Pd catalysts synthesis in this study.

Graphite oxide was first obtained following a modified Hummers methods previously reported by our group [30]. The graphite oxide was then rapidly exfoliated to obtain graphene via a thermal treatment at 1050 °C under Ar atmosphere. NGN was prepared by post heating the graphene under high purity ammonia mixed with Ar at 900 °C for 10 min.

2.2. Preparation of Pd, PdPt and Pt catalysts supported on NGN

2.2.1. NGN supported Pd catalysts

85.7 mg K_2PdCl_4 was dissolved into 2 mL H_2O and 134 mg NGN was dispersed into 170 mL H_2O under ultrasonication for 30 minutes. Then the K_2PdCl_4 solution was added into NGN-containing solution and ultrasonicated for 5 minutes to form a homogeneous mixture. After 1 hour of reaction under magnetic agitation at room temperature, 1 mL of the mixture was centrifuged and the supernatant liquid still showed light yellow colour, indicating that only a small amount of Pd precursor has not been reduced. Then, 1 mL ethylene glycol (EG) was added into the mixture to further reduce the Pd salt at 75 °C for 1 hour. Finally the mixture was centrifuged, fully washed and vacuum dried at 70 °C for 3 hours. The sample was denoted as NGN/Pd, in which the nominal Pd content is 17 wt. %.

2.2.2. NGN supported PdPt catalysts

42.8 mg K_2PtCl_4 was dissolved in 2 mL H_2O and 28 mg NGN/Pd was dispersed in 30 mL EG. Then calculated amount of K_2PtCl_4 aqueous solution was transferred to mix with NGN/Pd in EG under ultrasonication for 20 minutes, and the obtained mixture was heated at 70 °C for 1 hours to reduce the Pt precursor. It is noteworthy herein that the Pd nanoparticles on NGN/Pd were expected to act as seeds for subsequent seed-mediated Pt deposition [31,32]. The reaction temperature was prescribed according to our preliminary tests, in which we found that it takes nearly 1 hour for K_2PtCl_4 to be reduced by EG at 70 °C. With Pd seeds available, the Pt reduction prefers happening quickly on Pd surface. After reaction finished, the samples were centrifuged, washed and vacuum dried. Finally four samples were obtained and denoted as NGN/PdPt-x (x = 1, 2, 3, 4). The Pd/Pt mass ratio was designed to be 100:100, 100:50, 100:10 and 100:1 for NGN/PdPt-1, NGN/PdPt-2, NGN/PdPt-3 and NGN/PdPt-4, respectively.

2.2.3. NGN supported Pt catalysts

Pt nanoparticles were deposited on NGN using EG reduction method [33]. Briefly, 40 mg NGNs was ultrasonically dispersed in 100 mL EG solution containing 0.1 mol L^{-1} NaOH and 27 mg $H_2PtCl_6{\cdot}6H_2O$ for 10 min. The obtained mixture was refluxed at 160 °C for 3 h. After filtering and washing, the obtained catalyst was dried in a vacuum oven at 70 °C. The sample was denoted as NGN/Pt and the nominal Pt content is 20 wt.%.

2.3. Physical characterization of NGN/Pd, NGN/PdPt-x and NGN/Pt

The X-ray diffraction (XRD) patterns of all the samples were recorded on a Bruker D8 Advance X-ray diffractometer using Cu-Ka as the radiation source. The sample morphology was observed using field emission scanning electron microscope (SEM, Hitachi S4800) coupled with an energy dispersive X-ray spectroscopy (EDX) to analyze the composition.

2.4. Electrochemical characterization of NGN/Pd, NGN/PdPt-x and NGN/Pt

Catalysts inks were first prepared for coating on a glassy carbon (GC, Φ = 5 mm) electrode. Specifically, 2 mg NGN/Pd was mixed with 900 uL ethanol containing 4.4 mg Nafion® and ultrasonicated for 30 minutes to form uniform NGN/Pd ink, then 15 μL ink was pipetted onto the GC electrode and dried using an infrared lamp. The nominal loading of NGN/Pd on the GC electrode is 0.033 mg. For direct comparing the cyclic voltammograms (CVs) of NGN/PdPt-x and NGN/Pd, the NGN content in NGN/PdPt-x inks were kept constant like that in NGN/Pd ink. By doing thus, the loading of NGN and Pd for each catalyst on the GC electrode is similar and the difference of Pt content in NGN/PdPt-x can be well reflected from the CVs.

A three-electrode cell coupled with an Autolab potentiostat/galvanostat (Model PGSTAT-30, Ecochemie, Brinkman Instrument) was used for electrochemical characterization. A GC electrode, a Pt wire electrode and a saturated calomel electrode (SCE) were used as the working electrode, counter electrode and reference electrode, respectively. All potentials herein were referred to SCE, and all the electrochemical experiments were conducted at 25 °C in a N_2 saturated solution.

Cyclic voltammetry was first conducted at 50 mV s^{-1} on each catalyst in KOH solution and stable CVs were recorded. LSV was conducted at 5 mV s^{-1} to investigate the hydroxyl group (OH) formation because OH is believed to participate in alcohol oxidation [34,35]. Stable CVs were then recorded for methanol or ethanol oxidation on each catalyst, followed by corresponding chronoamperometry conducted at -0.3 V to reflect the poisoning effect during alcohol oxidation.

3. Results and Discussion

3.1. Structural characterizations for NGN/Pd, NGN/PdPt-x and NGN/Pt

The morphologies of the prepared catalysts were observed using SEM and the corresponding EDX spectra were recorded, as shown in Fig. 1. The Pd particles are homogeneously distributed on NGN (Fig. 1(a)), the average size of Pd nanoparticles is evidently larger than that of Pt nanoparticles (Fig. 1(b)), and the presence of Pd and Pt on NGN were confirmed by the corresponding EDX spectra shown in Fig. 1(c) and Fig. 1(d). From the EDX spectra for NGN/PdPt-1 and NGN/PdPt-2 in Fig. 1(e) and Fig. 1(f) we can see two distinct peaks ascribed to Pd and Pt. The height of the Pd and Pt peaks are similar in NGN/PdPt-1, while the height of Pd peak is nearly two times that of Pt peak in NGN/PdPt-2, consistent with the designed composition of 100:100 and 100:50. In fact, we also recorded the EDX spectra for NGN/PdPt-3 and NGN/PdPt-4, but the Pt signals were not detected because of the low Pt content in the two samples.

The XRD patterns of the six catalysts, namely NGN/Pd, NGN/PdPt-x and NGN/Pt, are shown in Fig. 2. There is a diffraction peak at about 26° existing in the XRD patterns of the six catalysts, corresponding to the carbon (002) plane diffraction [36]. The XRD pattern of NGN/Pt shows three Pt peaks, namely Pt(111) at 38.7°, Pt (220) at 67.3° and Pt(331) at 80.8° [36]. The main peak at 38.7° is broadened, indicating the small grain size of Pt in NGN/Pt. For the XRD patterns of NGN/Pd and NGN/PdPt-x, four peaks at 39.9°, 46.6°, 68.0° and 82.0° related to Pd(111), Pd(200), Pd(220) and Pd (311) planes diffraction [37] are relatively narrow and strong, indicating excellent crystal structures. Comparing the XRD patterns of NGN/Pd and NGN/PdPt-x, we can see that there are no distinct peaks that can be ascribed to Pt and four Pd peaks gradually get broadened, supporting the possibility that Pt was successfully deposited on Pd with increasing amount.

As described in the experimental section, the Pt deposition was induced by Pd nanoparticles on NGN/Pd, aiming to form Pt-on-Pd structure with changing surface composition. To show the corresponding surface structure of these catalysts, CVs were recorded for NGN/Pd, NGN/PdPt-x and NGN/Pt in 1 M KOH solution

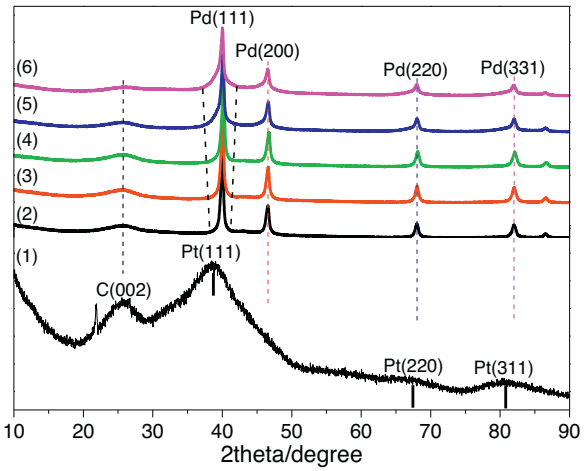

Fig. 2. XRD patterns for (1) NGN/Pt, (2) NGN/Pd, (3) NGN/PdPt-4, (4) NGN/PdPt-3, (5) NGN/PdPt-2 and (6) NGN/PdPt-1.

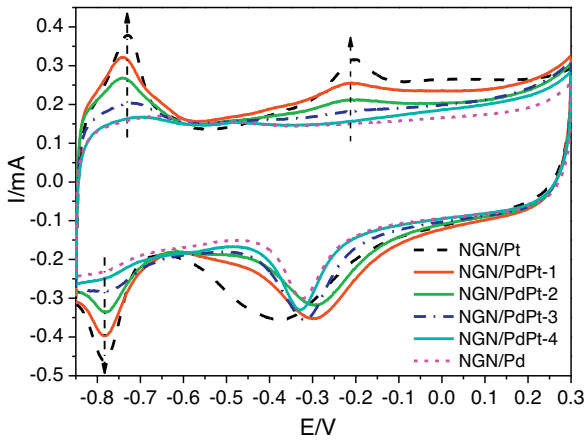

Fig. 3. CVs for NGN/Pt, NGN/Pd and NGN/PdPt-x recorded in 1 M KOH solution at 50 mV s^{-1}.

(Fig. 3). For the CVs of NGN/Pd, the weak H adsorption/desorption peak within the H range (-0.85 V ~ -0.60 V) and an evident peak at about -0.33 V related with Pd oxide reduction indicates the Pd presence in NGN/Pd. With Pt content increasing in the NGN/PdPt-x samples, the H adsorption and desorption features get increasingly distinct, indicating an increasing Pt proportion in the catalysts surfaces.

In addition, a peak at about -0.21 V in the anodic scan gradually appears with increasing strength, which can be ascribed to the adsorption of hydroxyl groups (OH) on the catalysts surfaces. It is noteworthy that the double layer region between the H region and the OH adsorption region becomes less discernible with increasing Pt content. This is because the Pt-OH formation can occur at a lower potential in comparison with Pd-OH. At the same time, the oxides reduction peak at about -0.3 V gets gradually broadened, indicating that the electrochemical active surface area increases with Pt content. Comparing the CVs of NGN/Pt with NGN/PdPt-x, the four peaks in NGN/Pt (H adsorption, H desorption, OH formation, and Pt oxide reduction) are all stronger than their counterparts for NGN/PdPt-x, indicating a higher electrochemical surface area in NGN/Pt possibly because of the smaller Pt size (see Fig. 1(b)) and slightly higher Pt loading.

It is noteworthy that we tried to observe the fine structure using high resolution transmission electron microscopy (HRTEM) but failed because (i) Pt and Pd are very similar in terms of lattice constant, making it difficult to observe the Pt and Pd lattice distance; and (ii) the Pd particles in NGN/Pd are not uniformly sized, making it difficult to observe the change of particles size after Pt deposition on Pd. However, the XRD and CV results indeed proved that Pt successfully deposited on NGN/Pd with increasing Pt surface ratios.

3.2. Electrochemical characterization for NGN/Pd, NGN/PdPt-x and NGN/Pt

Since the alcohol oxidation activity is closely related with the OH formation property of a catalyst [34,35], the LSV curves for OH formation on NGN/Pd, NGN/PdPt-x and NGN/Pt were recorded in 0.1 M and 1 M KOH solutions (Fig. 4) to better understand the alcohol oxidation behaviour of these catalysts. For the LSV curve of NGN/Pd, a peak occurring at about -0.4 V in 1 M KOH solution can

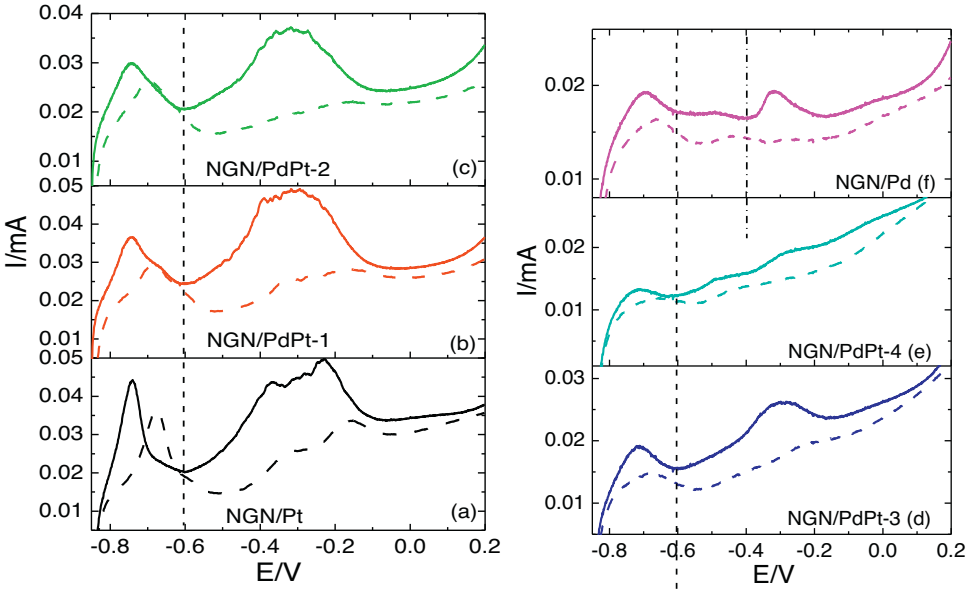

Fig. 4. LSV curves for NGN/Pt, NGN/Pd and NGN/PdPt-x recorded at 5 mV s^{-1} in 0.1 M KOH (dashed line) and 1 M KOH solution (solid line).

be ascribed to Pd-OH formation while the Pd-OH formation in 0.1 M KOH solution is not as distinguished as in 1 M KOH solution. This means that the KOH participates in the Pd-OH formation, which is not as pronounced with a lower KOH concentration of 0.1 M. For the LSV curves of NGN/PdPt-x in 1 M KOH, the OH formation starts at a lower potential (about -0.6 V) in comparison with -0.4 V for NGN/Pd, and the peak for OH formation gets increasingly broadened and more intense due to the increasing Pt content. Furthermore, the OH formation on NGN/PdPt-x (x = 1, 2, 3) in 0.1 M KOH is evident from the peaks at about -0.2 V, indicating facile kinetics for OH formation on Pt surface compared with Pd surface. Especially for NGN/PdPt-1, with theoretically equal Pt and Pd mass content, the OH formation current was greatly enhanced in comparison with NGN/Pd (the Pd loading in NGN/PdPt-1 and NGN/Pd is the same), further indicating that Pt is more prone to binding OH than Pd. Comparing the LSV curve of NGN/PdPt-1 with that of NGN/Pt, we can see that the two profiles are quite similar, suggesting that the surface properties of NGN/PdPt-1 are dominated by Pt component.

The catalytic properties of NGN/Pd, NGN/PdPt-x, and NGN/Pt for methanol and ethanol oxidation were compared using CV method, as shown in Fig. 5(a-f). By making such a comparison, we aimed to address two issues: (1) the intrinsic activity of Pt and Pd; and (2) the reason why Pd has lower activity towards methanol oxidation compared with ethanol oxidation. To compare the intrinsic activity of Pt and Pd for alcohol oxidation, onset potential (E_{onset}) is commonly used as an indicator [6]. However, it is difficult to precisely compare the E_{onset} on two catalysts, especially when there is a considerable difference in the currents for two catalysts. Therefore, we use the half-wave potential ($E_{1/2}$) of ethanol

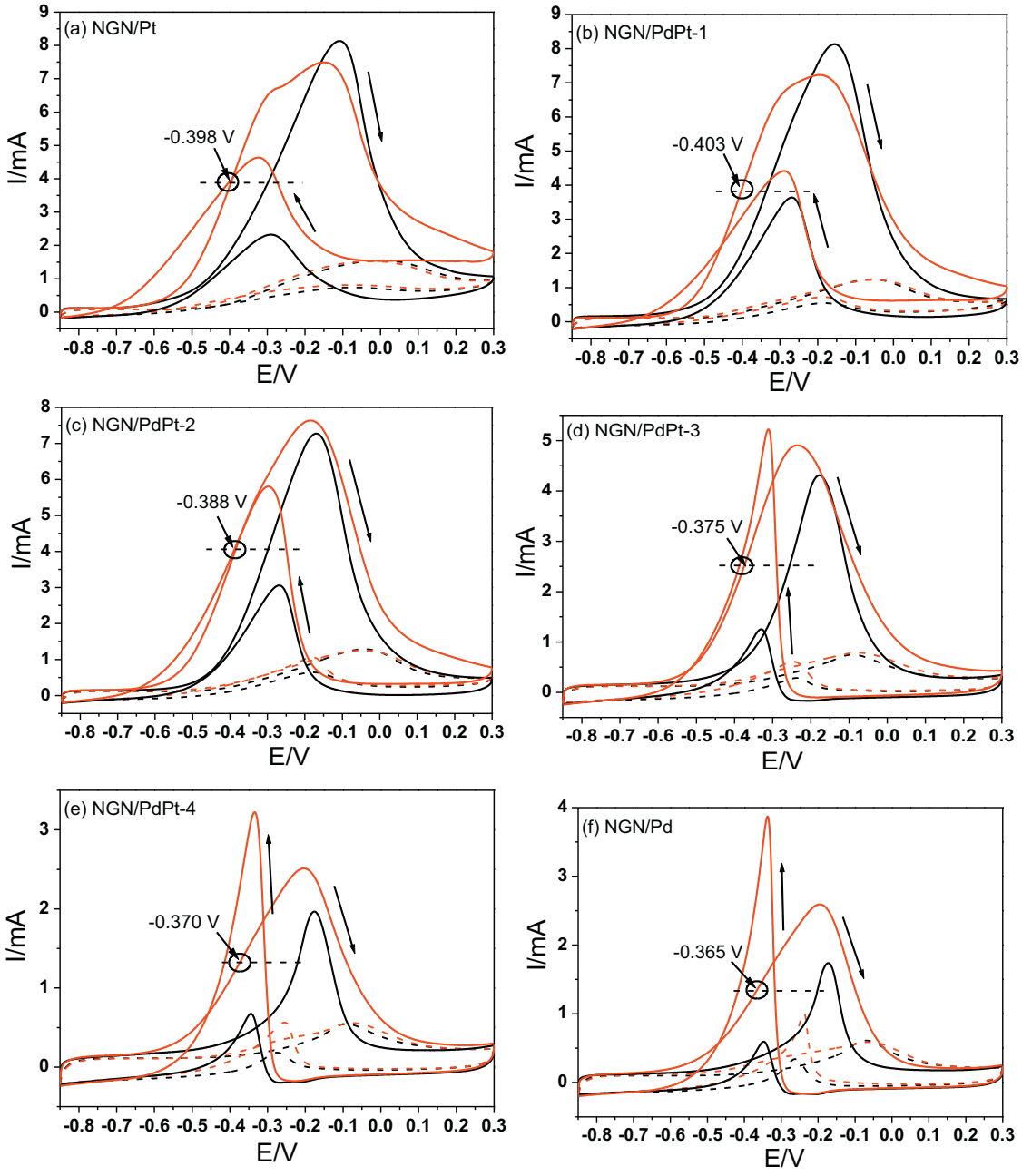

Fig. 5. CVs for NGN/Pt, NGN/Pd and NGN/PdPt-x recorded at 50 mV s^{-1} in 0.1 M KOH (dashed line) and 1 M KOH (solid line) solution containing 1 M methanol (black line) and 1 M ethanol (red line).

oxidation to make the comparison in this study. The basic consideration of using $E_{1/2}$ is that if the peak current is of a same value on two catalysts, the lower $E_{1/2}$ means a lower overpotential and correspondingly faster kinetics. From the $E_{1/2}$ values marked on CVs of the catalysts in Fig. 5, we can see that Pd has the highest $E_{1/2}$ (-0.365 V) and the $E_{1/2}$ shifts to lower potentials with increasing Pt content, indicating that the ethanol oxidation on Pt is kinetically more facile than on Pd. Others have reported that Pd is more active for ethanol oxidation than Pt according to a lower E_{onset} on Pd/C (-0.52 V) than on Pt/C (-0.51 V) together with a higher current on Pd/C at -0.3 V (see Table 1 in Ref. 6). In fact, the $E_{1/2}$ on Pt is evidently lower than that on Pd/C (see Fig. 7 in Ref. 6), indicating that Pt is intrinsically more active than Pd for ethanol oxidation. In a comparison made between Pd and Pt [23], the $E_{1/2}$ for ethanol oxidation on Pd is found to be higher than on Pt (see Fig. 3 in Ref. 23). Such a difference can also be noticed in a report by Aarnio [5], which is in good agreement with our present results. In fact, we also found indirect support for our judgement based upon the H-D kinetic isotope effects of ethanol oxidation on Pt and Pd [24]. The study demonstrated that the breaking of C-H bond at á-site is the rate-determining step (RDS) for ethanol oxidation on Pd and this step is faster on Pt, indirectly reflecting the higher activity of the latter.

The $E_{1/2}$ values of methanol oxidation on each of the catalysts follow a similar trend as those of ethanol oxidation. For example, the $E_{1/2}$ of methanol oxidation on NGN/Pd is about -0.23 V while that on NGN/Pt is about -0.29 V, indicating Pt is more active than Pd for ethanol oxidation as well as methanol oxidation. These results are in good agreement with the reports by Bunazawa [38] and Xu [6]. For methanol oxidation in Xu's report, the E_{onset} is -0.38 V on Pd/C while -0.52 V on Pt/C, and the $E_{1/2}$ is about -0.11 V on Pd/C while -0.25 V on Pt/C, indicating a higher activity of Pt than Pd.

As for the second topic, namely, the reason why Pd has lower activity towards methanol oxidation than ethanol oxidation, we can find hints in the reaction mechanism of alcohols oxidation. As mentioned above, the breaking of C-H at the á-site is believed to be the RDS for ethanol oxidation on Pd [24]. In fact, this step can also be assumed to be the RDS for methanol oxidation, as verified by in situ infrared spectroscopy technology [39]. Since the C-H bond at the á-site in methanol is stronger than in ethanol [20], it is understandable that methanol oxidation activity should be lower than ethanol oxidation activity, as has been previously observed on an Au surface [20].

As other researchers have reported [6–8], we indeed observed that Pd catalyst has a lower activity towards methanol oxidation than ethanol oxidation, as shown in Fig. 5. The peak current of methanol oxidation is clearly lower than that of ethanol oxidation on NGN/Pd and the forward scan curve for the former is right shifted in comparison with the latter. In fact, such a shift can be noticed on all the six catalysts, indicating a lower activity of methanol oxidation compared with ethanol oxidation, regardless of whether on Pd or Pt surface.

Table 1
The deactivation extent of different catalysts during ethanol oxidation (red) and methanol oxidation (blue). (For interpretation of the references to colour in this table legend, the reader is referred to the web version of this article.)

	I_t(M) /mA	I_t(E) /mA	I_{CV}(M) /mA	I_{CV}(E) /mA	I_t(M)/I_{CV}(M)	I_t (E)/I_{CV}(E)
NGN/Pt	1.72	0.29	3.8	6.5	45%	4.5%
NGN/PdPt-1	1.15	0.23	4.9	6.6	23%	3.5%
NGN/PdPt-2	0.62	0.16	2.7	5.7	23%	2.8%
NGN/PdPt-3	0.31	0.35	1.4	4.0	22%	8.8%
NGN/PdPt-4	0.11	0.17	0.46	1.8	24%	9.4%
NGN/Pd	0.11	0.19	0.41	1.8	27%	10.5%

To quantitatively compare the shifts of forward scan curves for methanol and ethanol oxidation on the six catalysts, we first determined the half height of the ethanol oxidation peak current on each catalyst. At this current, we then obtained the potential for methanol oxidation (E_M) and ethanol oxidation (E_E) from the forward scan curves, as exemplified in Fig. 5(f). Finally the differences in potential (E_M-E_E) was calculated for all the catalysts and illustrated in the upper graph in Fig. 6(a). We also noticed from Fig. 5 that the ratios of methanol oxidation peak current (I_M) to ethanol oxidation peak current (I_E) are different on the six catalysts, as illustrated in the lower graph in Fig. 6(a). From Fig. 6(a) we can see that the values of E_M-E_E and I_E/I_M on NGN/Pd are the highest compared with other catalysts. With increasing the Pt content, the value of E_M-E_E and I_E/I_M on NGN/PdPt-x decreased linearly. Herein we assume that the value of E_M-E_E and I_E/I_M on a catalyst are related with different activity of methanol and ethanol oxidation, then it is imaginable that the difference in activity of methanol and ethanol can be levelled by an extremely active catalyst (levelling effect) or magnified by a less active catalyst (differentiating effect). Conversely, the value of E_M-E_E and I_E/I_M can be used to reflect the intrinsic activities of different catalysts. As seen in Fig. 6(a), the value of E_M-E_E on NGN/PdPt-x decreased linearly with increasing Pt content in comparison with NGN/Pd, and the value of I_E/I_M decreased to nearly 1 for NGN/Pt (meaning a levelling effect), indicating that Pt is more active than Pd for alcohols oxidation. Based upon the above results, we can point to two reasons for lower Pd activity towards methanol oxidation than ethanol oxidation. First, Pd is a less active catalyst than Pt, and second, methanol oxidation is kinetically less favourable than ethanol oxidation.

As is well known, surface OH species form through electrosorption of hydroxide (OH^-) and then participates in alcohol oxidation [35]. Since Pt is more prone to binding OH than Pd (see Fig. 4), we can deduce that a similar increase in OH^- concentration would produce a greater enhancement of alcohol oxidation current on Pt than on Pd. By analysing the data from CVs in Fig. 5, we found that this deduction was proved to be true, as shown in Fig. 6 (b). The I_{1M} (or $I_{0.1M}$) represents the peak current of alcohol oxidation in 1 M KOH (or 0.1 M KOH) while the ratio of I_{1M} to $I_{0.1M}$ represents the degree of activity enhancement by an increase of KOH concentration. It can be seen that the ratio of I_{1M} to $I_{0.1M}$ is the lowest for NGN/Pd, for both methanol and ethanol oxidation. With increasing Pt content in NGN/PdPt-x, the corresponding ratio increases linearly, supporting the conclusion that Pt has a higher affinity for reactive OH species in comparison with Pd.

As shown from the CVs in Fig. 5, the $E_{1/2}$ for ethanol oxidation on NGN/PdPt-1 is the lowest among all the $E_{1/2}$ values and the corresponding current at $E_{1/2}$ for ethanol oxidation on NGN/PdPt-1 is far higher than that on NGN/Pd. However, the potentiostatic current of ethanol oxidation on NGN/PdPt-1 obtained from the chronoamperometry tests (see Fig. 7) is not considerable higher than, but rather, nearly the same as that on NGN/Pd. This indicates that the Pt surface, in comparison with Pd, is prone to deactivation during ethanol oxidation. On the other hand, although the potentiodynamic currents at -0.3 V for methanol oxidation are all smaller than the ethanol oxidation currents on NGN/Pt, NGN/PdPt-1 and NGN/PdPt-2 (see Fig. 5), the corresponding potentiostatic currents for methanol oxidation are, surprisingly, notably higher than the ethanol oxidation currents (see Fig. 7), indicating that the poisoning effect of ethanol oxidation is stronger than methanol oxidation. To clearly analyze the poisoning phenomena, we listed the relevant data together with necessary calculations, as shown in Table 1. The I_t(M) and I_t(E) in Table 1 represent the ending currents for methanol and ethanol oxidation during potentiostatic tests at -0.3 V. I_{CV}(M) and I_{CV}(E) represent the corresponding currents at -0.3 V obtained from the CVs in Fig. 5, and the ratio of

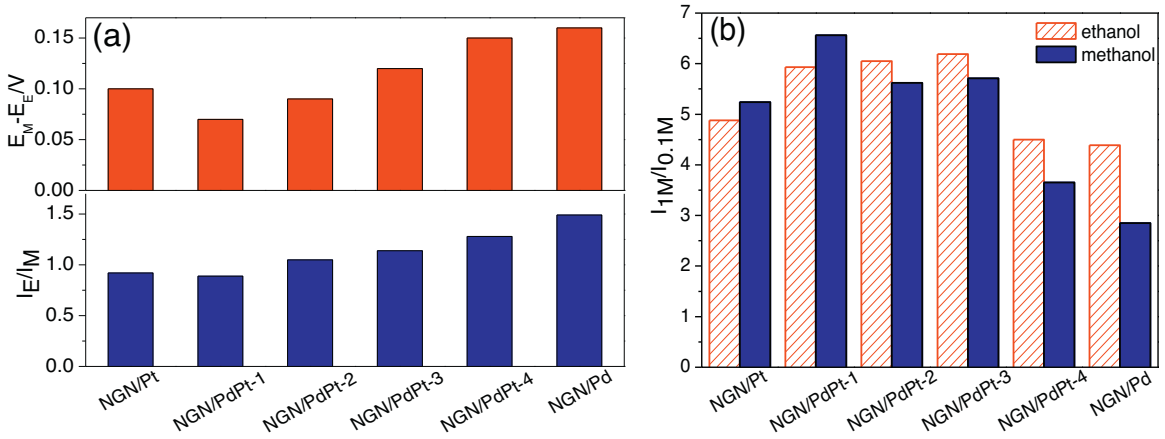

Fig. 6. (a) the changing trend of the values of E_M-E_E (upper graph) and I_E/I_M (lower graph) for NGN/Pt, NGN/Pd and NGN/PdPt-x collected from Fig. 5; (b) the changing ratio of I_{1M} to $I_{0.1M}$ for NGN/Pt, NGN/Pd and NGN/PdPt-x collected from Fig. 5.

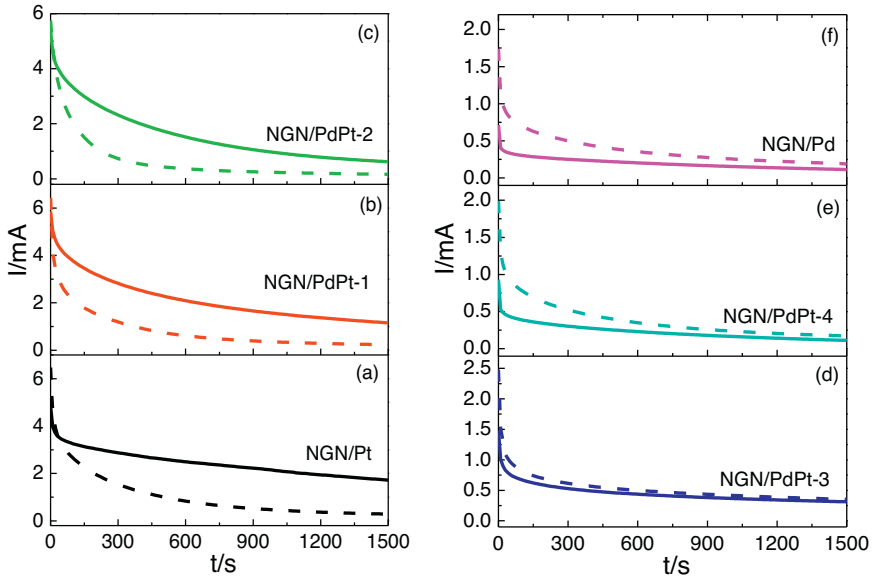

Fig. 7. Chronoamperometry curves for NGN/Pt, NGN/Pd and NGN/PdPt-x recorded at −0.3 V in 1 M KOH solution containing 1 M methanol (solid line) and ethanol (dashed line).

$I_t(M)/I_{CV}(M)$ or $I_t(E)/I_{CV}(E)$ [9] reflects the poisoning effect of methanol or ethanol oxidation on different catalysts. The values of $I_t(E)/I_{CV}(E)$ in Table 1 are lower than the values of $I_t(M)/I_{CV}(M)$ on all catalysts, indicating that the poisoning effect of ethanol oxidation is higher than methanol oxidation. On the other hand, the value of $I_t(E)/I_{CV}(E)$ for NGN/Pd is higher than the values for NGN/Pt and NGN/PdPt-x (which contain Pt), indicating that Pd is less prone to deactivation than Pt during ethanol oxidation. In particular, the values of $I_t(E)/I_{CV}(E)$ for NGN/Pt, NGN/PdPt-1 and NGN/PdPt-2 are evidently lower than the values for NGN/PdPt-3 and NGN/PdPt-4, indicating a greater extent of deactivation in the former three catalysts. Because the Pt content in the former three catalysts are evidently higher than in the latter two catalysts, this result further confirmed that Pt is more prone to deactivation than Pd during ethanol oxidation.

The severe Pt deactivation during ethanol oxidation has been widely reported [23,25,26], however, there is still no consensus as to the reason for the deactivation. One common explanation for this deactivation is that the C_1 species [23] formed through the C-C cleavage of ethanol is responsible for this poisoning. However, many researchers using in-situ methods have proven that the acetaldehyde-acetate route is the dominant pathway for ethanol oxidation in alkaline media, regardless of whether on a Pt or Pd surface [17,18,40]. Recently, first principles calculations were used to support the finding that the cleavage of C-H at á-site is the main mechanism for ethanol oxidation on Pd, with the main product being acetaldehyde and acetate [34]. It is noteworthy that although CO_2 formation has been detected by in-situ Fourier transform infrared spectroscopy (FTIR) method to support C-C cleavage during ethanol oxidation on Pd, the main product was found to be acetate [41], indicating that ethanol oxidation mainly proceeds via the acetaldehyde-acetate route. On the other hand, a phenomenon of pH decrease in the thin layer solution during FTIR measurement has been reported and the decreased pH is believed to facilitate the formation of C_1 species [17,18,39,41]. Therefore, the C_1 signal detected in low pH environment during FTIR measurement cannot corroborate the C-C cleavage mechanism.

Assuming that the acetaldehyde-acetate route is the major mechanism for ethanol oxidation in alkaline media, the deactivation of Pt during ethanol oxidation can be ascribed to acetaldehyde

[25]. Specifically, because acetaldehyde can readily polymerize through an aldol condensation [5,25] in alkaline media, the polymerization might adsorb onto the surface and poison the catalyst. On the other hand, it should be easier for methanol oxidation to produce C_1 species than ethanol oxidation since the latter involves complex C-C breaking. If it is the C_1 species that poisons the Pt surface, then more severe Pt deactivation should occur during methanol oxidation compared with ethanol oxidation. In fact, more severe Pt deactivation was observed during ethanol oxidation, indicating that the true poisoning species during ethanol oxidation is not the C_1 species and that the most acceptable explanation for the deactivation is aldol condensation.

Based upon this deactivation mechanism, we can understand why the poisoning effect of ethanol oxidation is stronger than methanol oxidation. For methanol oxidation in alkaline media, formaldehyde-formate route has been proven to be the dominant process [5,42]. Since formaldehyde cannot undergo aldol condensation, there is no chance of polymerization that deactivates the catalysts. Therefore the poisoning effect of methanol oxidation is less severe than ethanol oxidation.

Although both Pt and Pd activity can be poisoned during ethanol oxidation, the extent of Pd deactivation is smaller than that of Pt deactivation, as shown in Table 1. Considering that Pt is more active than Pd, it might seem a coincidence that Pt also loses activity more quickly. Recently, Buso-Rogero et. al [25] investigated the deactivation of a Pt single-crystal electrode during ethanol oxidation in alkaline media and found that the Pt(111) electrode exhibits the highest activity for ethanol oxidation and simultaneously the highest deactivation rate. The authors believed that a higher activity of Pt(111) for ethanol oxidation means faster production of acetaldehyde, and correspondingly faster deactivation. Herein we assume that the faster deactivation of NGN/Pt together with NGN/PdPt-1 and NGN/PdPt-2 during ethanol oxidation is also a direct result of the higher activity of Pt, but not a coincidence. Although acetaldehyde can be oxidized to acetate [43], the rate of acetaldehyde production on highly active Pt might be faster than the rate of subsequent acetaldehyde oxidation, so the aldol condensation would proceed with strong poisoning effect. However, the rate of acetaldehyde production on modestly active Pd is likely not as fast and most acetaldehyde can be immediately oxidized to acetate, thus the deactivation rate of Pd is shown to be modest.

Based upon the above discussion, we know that although methanol oxidation is kinetically less favourable than ethanol oxidation, the poisoning effect of methanol oxidation is less severe. Therefore, if high Pt utilization can be achieved with simultaneously excellent activity, methanol can be used as a competitive fuel for ADAFCs. On the other hand, the efficiency of ethanol utilization is quite low because ethanol oxidation is incomplete during the acetaldehyde-acetate route, and ethanol also poses apparent poisoning effect on Pd catalyst. Therefore, for ethanol oxidation in alkaline media, an ideal catalyst should be able to break the C-C bond in the ethanol molecule. If that criterion could be met, the efficiency of ethanol utilization could be improved and the acetaldehyde deactivation could be avoided.

4. Conclusion

Six catalysts with different ratio of Pt/Pd were designed and investigated. Electrochemical characterization showed that Pt is intrinsically more active than Pd for methanol and ethanol oxidation but that Pt deactivation is more severe during ethanol oxidation compared with Pd. Ethanol oxidation is kinetically more favourable than methanol oxidation on both Pt and Pd surface, but the poisoning effect of ethanol oxidation is more severe than methanol oxidation. Concerning catalyst design, ideal catalysts for methanol oxidation in alkaline media should be Pt-based catalysts in which the Pt component should be highly utilized. For ethanol oxidation, excellent catalysts should be able to fulfill the complete oxidation of ethanol through a C-C cleavage mechanism.

Acknowledgments

This research is financially supported by the National Natural Science Foundation of China (U1304215) and the China Scholarship Council (201308410311). This research was also supported by Natural Sciences and Engineering Research Council of Canada (NSERC), Canada Research Chair (CRC) Program, Canada Foundation for Innovation (CFI), and the University of Western Ontario.

References

[1] S.H. Sun, G.X. Zhang, N. Gauquelin, N. Chen, J.G. Zhou, S.L. Yang, W.F. Chen, X.B. Meng, D.S. Geng, M.N. Banis, R.Y. Li, S.Y. Ye, S. Knights, G.A. Botton, T.K. Sham, X. L. Sun, Single-atom catalysis using Pt/graphene achieved through atomic layer deposition, Sci. Rep. 3 (2013) 1775.
[2] A. Sadiki, P. Vo, S.Z. Hu, T.S. Copenhaver, L. Scudiero, S. Ha, J.L. Haan, Increased electrochemical oxidation rate of alcohols in alkaline media on palladium surfaces electrochemically modified by antimony, lead, and tin, Electrochimi. Acta 139 (2014) 302.
[3] J.J. Li, J.S. Wang, X. Guo, J.H. Zhao, C.Y. Song, L.C. Wang, Improving the stability and ethanol electro-oxidation activity of Pt catalysts by selectively anchoring Pt particles on carbon-nanotubes-supported-SnO_2, Fuel Cell 12 (2012) 898.
[4] Y.Z. Su, M.Z. Zhang, X.B. Liu, Z.Y. Li, X.C. Zhu, C.W. Xu, S.P. Jiang, Development of Au promoted Pd/C electrocatalysts for methanol, ethanol and isopropanol oxidation in alkaline medium, Inter. J. Electrochem. Sci. 7 (2012) 4158.
[5] A. Santasalo-Aarnio, Y. Kwon, E. Ahlberg, K. Kontturi, T. Kallio, M.T.M. Koper, Comparison of methanol, ethanol and iso-propanol oxidation on Pt and Pd electrodes in alkaline media studied by HPLC, Electrochem. Commun. 13 (2011) 466.
[6] C.W. Xu, L.Q. Cheng, P.K. Shen, Y.L. Liu, Methanol and ethanol electrooxidation on Pt and Pd supported on carbon microspheres in alkaline media, Electrochem. Commun. 9 (2007) 997.
[7] P.K. Pandey, V. Lakshminarayanan, Electro-oxidation of formic acid, methanol, and ethanol on electrodeposited Pd-polyaniline nanofiber films in acidic and alkaline medium, J. Phys. Chem. C 113 (2009) 21596.
[8] L.Z. Li, M.X. Chen, G.B. Huang, N. Yang, L. Zhang, H. Wang, Y. Liu, W. Wang, J.P. Gao, A green method to prepare PdeAg nanoparticles supported on reduced graphene oxide and their electrochemical catalysis of methanol and ethanol oxidation, J. Power Sources 263 (2014) 13.
[9] Z.Y. Zhang, L. Xin, K. Sun, W.Z. Li, Inter. Pd-Ni electrocatalysts for efficient ethanol oxidation reaction in alkaline electrolyte, J. Hydrogen Energy 36 (2011) 12686.
[10] E. Antolini, E.R. Gonzalez, Alkaline direct alcohol fuel cells, J. Power Sources 195 (2010) 3431.
[11] E.L. Reddy, J. Karuppiah, H.C. Lee, D.H. Kim, Steam reforming of methanol over copper loaded anodized aluminum oxide (AAO) prepared through electrodeposition, J. Power Sources 268 (2014) 88.
[12] Z.J. Wang, C.X. Wang, S.Q. Chen, Y. Liu, Co-Ni bimetal catalyst supported on perovskite-type oxide for steam reforming of ethanol to produce hydrogen, Inter. J. Hydrogen Energy 39 (2014) 5644.
[13] L. Zhang, H.B. Wu, Y. Yan, X. Wang, X.W. Lou, Hierarchical MoS_2 microboxes constructed by nanosheets with enhanced electrochemical properties for lithium storage and water splitting, Energy Environ. Sci. 7 (2014) (2014) 3302.
[14] L. Kuai, J. Geng, C.Y. Chen, E.J. Kan, Y.D. Liu, Q. Wang, B.Y. Geng, A reliable aerosol-spray-assisted approach to produce and optimize amorphous metal oxide catalysts for electrochemical water splitting, Angew. Chem. Int. Ed. 53 (2014) 7547.
[15] Y.J. Wang, J.L. Qiao, R. Baker, J.J. Zhang, alkaline polymer electrolyte membranes for fuel cell applications, Chem. Soc. Rev. 42 (2013) 5768.
[16] S.Y. Shen, T.S. Zhao, Q.X. Wu, Inter. Product analysis of the ethanol oxidation reaction on palladium-based catalysts in an anion-exchange membrane fuel cell environment, J. Hydrogen Energy 37 (2012) 575.
[17] Z.Y. Zhou, Q. Wang, J.L. Lin, N. Tian, S.G. Sun, In situ FTIR spectroscopic studies of electrooxidation of ethanol on Pd electrode in alkaline media, Electrochimi. Acta 55 (2010) 7995.
[18] P.A. Christensen, S.W.M. Jones, A. Hamnett, In situ FTIR studies of ethanol oxidation at polycrystalline Pt in alkaline solution, J. Phys. Chem. C 116 (2012) 24681.
[19] S. Beyhan, K. Uosaki, J.M. Feliu, E. Herrero, Electrochemical and in situ FTIR studies of ethanol adsorption and oxidation on gold single crystal electrodes in alkaline media, J. Electroanal. Chem. 707 (2013) 89.
[20] Y. Kwon, S.C.S. Lai, P. Rodriguez, M.T.M. Koper, Electrocatalytic oxidation of alcohols on gold in alkaline media: base or gold catalysis? J. Am. Chem. Soc. 133 (2011) 6914.
[21] F. Gobal, Y. Valadbeigi, L.M. Kasmaee, On the significance of hydroxide ion in the electro-oxidation of methanol on Ni, J. Electroanal. Chem. 650 (2011) 219.

[22] M.Q. Yu, S.L. Wang, J.Y. Hu, Z.Y. Chen, Y.H. Bai, L.J. Wu, J.R. Chen, X.X. Weng, Additive-free macroscopic-scale synthesis of coral-like nickel cobalt oxides with hierarchical pores and their electrocatalytic properties for methanol oxidation, Electrochimi. Acta 145 (2014) 300.
[23] L. Ma, D.R. Chu, R.R. Chen, Inter. Comparison of ethanol electro-oxidation on Pt/C and Pd/C catalysts in alkaline media, J. Hydrogen Energy 37 (2012) 11185.
[24] J. Ren, Y.Y. Yang, B.W. Zhang, N. Tian, W.B. Cai, Z.Y. Zhou, S.G. Sun, H-D kinetic isotope effects of alcohol electrooxidation on Au Pd and Pt electrodes in alkaline solutions, Electrochem. Commun. 37 (2013) 49.
[25] C. Buso-Rogero, E. Herrero, J.M. Feliu, Ethanol oxidation on Pt single-crystal electrodes: surface-structure effects in alkaline medium, ChemPhysChem 15 (2014) 2019.
[26] S. Cherevko, X.L. Xing, C.H. Chung, Pt and Pd decorated Au nanowires: Extremely high activity of ethanol oxidation in alkaline media, Electrochimi. Acta 56 (2011) 5771.
[27] W.J. Lee, D.S. Choi, S.H. Lee, J. Lim, J.E. Kim, D.J. Li, G.Y. Lee, S.O. Kim, Electroless bimetal decoration on N-doped carbon nanotubes and graphene for oxygen reduction reaction catalysts, Part. Part. Syst. Char. 31 (2014) 965.
[28] H.J. Yin, H.J. Tang, D. Wang, Y. Gao, Z.Y. Tang, Facile synthesis of surfactant-free Au cluster/graphene hybrids for high-performance oxygen reduction reaction, ACS NANO 6 (2012) 8288.
[29] D.P. He, Y.L. Jiang, H.F. Lv, M. Pan, S.C. Mu, Nitrogen-doped reduced graphene oxide supports for noble metal catalysts with greatly enhanced activity and stability, Appl. Catal. B: Environ. 132–133 (2013) 379.
[30] D.S. Geng, Y. Chen, Y.G. Chen, Y.L. Li, R.Y. Li, X.L. Sun, S.Y. Ye, S. Knights, High oxygen-reduction activity and durability of nitrogen-doped graphene, Energy Environ. Sci. 4 (2011) 760.
[31] Y. Zhang, Y.C. Hsieh, V. Volkov, D. Su, W. An, R. Si, Y.M. Zhu, P. Liu, J.X. Wang, R.R. Adzic, High Performance Pt Mono layer Catalysts Produced via Core-Catalyzed Coating in Ethanol, ACS Catal. 4 (2014) 738.
[32] R. Choi, S.I. Choi, C.H. Choi, K.M. Nam, S.I. Woo, J.T. Park, S.W. Han, Designed synthesis of well-defined Pd@Pt core-shell nanoparticles with controlled Shell thickness as efficient oxygen reduction electrocatalysts, Chem. Eur. J. 19 (2013) 8190.
[33] N.C. Cheng, J. Liu, M.N. Banis, D.S. Geng, R.Y. Li, S.Y. Ye, S. Knights, X.L. Sun, High stability and activity of Pt electrocatalyst on atomic layer deposited metal oxide/nitrogen-doped graphene hybrid support, Inter. J. Hydrogen Energy 39 (2014) 15967.
[34] T. Sheng, W.F. Lin, C. Hardacre, P. Hu, Role of water and adsorbed hydroxyls on ethanol electrochemistry on Pd: new mechanism, active centers, and energetics for direct ethanol fuel cell running in alkaline medium, J. Phys. Chem. C 118 (2014) 5762.
[35] J.S. Wang, R.R. Shi, X. Guo, J.Y. Xi, J.H. Zhao, C.Y. Song, L.C. Wang, J.J. Zhang, Highly active Pt-on-Au catalysts for methanol oxidation in alkalinemedia involving a synergistic interaction between Pt and Au, Electrochimi. Acta 123 (2014) 309.
[36] P. Kannan, T. Maiyalagan, N.G. Sahoo, M. Opallo, Nitrogen doped graphene nanosheet supported platinum nanoparticles as high performance electrochemical homocysteine biosensors, J. Mater. Chem. B 1 (2013) 4655.
[37] B.P. Vinayan, R. Nagar, S. Ramaprabhu, Solar light assisted green synthesis of palladium nanoparticle decorated nitrogen doped graphene for hydrogen storage application, J. Mater. Chem. A 1 (2013) 11192.
[38] H. Bunazawa, Y. Yamazaki, Ultrasonic synthesis and evaluation of non-platinum catalysts for alkaline direct methanol fuel cells, J. Power Sources 190 (2009) 210.
[39] Y.Y. Yang, J. Ren, H.X. Zhang, Z.Y. Zhou, S.G. Sun, W.B. Cai, Infrared spectroelectrochemical study of dissociation and oxidation of methanol at a palladium electrode in alkaline solution, Langmuir 29 (2013) 1709.
[40] E. Guelzow, M. Beyer, K.A. Friedrich, S. Pengel, P. Fischer, H. Bettermann, Monitoring reactions in alkaline direct ethanol fuel cells assembled with non-Pt-catalyst, ECS Trans. 30 (2011) 345.
[41] X. Fang, L.Q. Wang, P.K. Shen, G.F. Cui, C. Bianchini, An in situ Fourier transform infrared spectroelectrochemical study on ethanol electrooxidation on Pd in alkaline solution, J. Power Sources 195 (2010) 1375.
[42] P.A. Christensen, D. Linares-Moya, The role of adsorbed formate and oxygen in the oxidation of methanol at a polycrystalline Pt electrode in 0.1M KOH: an in situ Fourier transform infrared study, J. Phys. Chem. C 114 (2010) 1094.
[43] Z.X. Liang, T.S. Zhao, J.B. Xu, L.D. Zhu, Mechanism study of the ethanol oxidation reaction on palladium in alkaline media, Electrochimi. Acta 54 (2009) 2203.